Applied Catalysis B: Environmental 166–167 (2015) 56–65

Contents lists available at ScienceDirect

Applied Catalysis B: Environmental

journal homepage: www.elsevier.com/locate/apcatb

Catalytic upgrading of sugar fractions from pyrolysis oils in supercritical mono-alcohols over Cu doped porous metal oxide

Wang Yin[a], Robertus Hendrikus Venderbosch[b], Giovanni Bottari[c], Krzysztof K. Krawzcyk[c], Katalin Barta[c,*], Hero Jan Heeres[a,**]

[a] Department of Chemical Engineering, University of Groningen, Nijenborgh 4, 9747 AG Groningen, The Netherlands
[b] Biomass Technology Group BV, Josink Esweg 34, 7545 PN Enschede, The Netherlands
[c] Stratingh Institute for Chemistry, University of Groningen, Nijenborgh 4, 9747 AG Groningen, The Netherlands

ARTICLE INFO

Article history:
Received 4 August 2014
Received in revised form 19 October 2014
Accepted 22 October 2014
Available online 31 October 2014

Keywords:
Pyrolysis oils
Sugar fractions
Cu-PMO
Supercritical methanol

ABSTRACT

In this work, we report on the catalytic valorization of sugar fractions, obtained by aqueous phase extraction of fast pyrolysis oils, in supercritical methanol (scMeOH) and ethanol (scEtOH) over a copper doped porous metal oxide (Cu-PMO). The product mixtures obtained are, in principle, suitable for direct co-feeding in methanol to hydrocarbon (MTH) processes, as fuel additives, or can be further fractionated or transformed to useful bulk chemicals. The main components of the obtained product mixtures in scMeOH are aliphatic mono-alcohols (51%), diols (22%), esters (15%), ethers (9%) and furanics (3%). Similar product suite is obtained by converting concentrated, 15 wt% sugar fractions with added 50 bar H_2 in scEtOH. The extensive depolymerization of the sugar polymers and oligomers contained in the sugar fraction is verified by gel permeation chromatography (GPC) and product stability upon catalytic treatment is confirmed by thermogravimetric analysis (TGA). In addition, model compound studies, using levoglucosan and D-cellobiose allow for more specific insight into the chemical pathways taking place during these transformations. The catalyst is characterized by various techniques, including XRD, NH_3-TPD, BET, and TEM. The stability of the catalyst using 5 wt% sugar fraction in scMeOH is also evaluated.

1. Introduction

Efficient catalytic methodologies for the valorization of renewable and CO_2-neutral lignocellulosic biomass have significant societal and environmental impact [1]. The concept of a biorefinery, which combines catalytic valorization of lignocelluloses with conventional refinery units, is an important potential strategy to obtain clean liquid fuels or useful chemicals from biomass [1–5].

Pyrolysis is an attractive approach for the conversion of lignocellulosic biomass to liquid energy carriers and is considered a key technology towards realization of the biorefinery concept [1,2]. Pyrolysis oils, obtained through high temperature treatment of biomass, are complex mixtures of various acids, alcohols, aldehydes, ketones, sugars as well as phenolics and lignin fractions [6,7]. Due to the presence of these reactive functional groups and their acidity (pH = ~2–3), pyrolysis oils are relatively unstable, viscous liquids. Upgrading procedures such as hydrodeoxygenation have been successfully applied [8–13], however these are frequently accompanied by competing side reactions, which lead to char formation and ultimately, decreased product yields. Similarly, direct co-feeding of pyrolysis oils [14] or stabilized pyrolysis oils [15] with crude oil for input into petroleum refinery infrastructures faces the common problem of coke deposition, where lignin, and lignin-derived phenolics contribute to repolymerization reactions [6,16].

Aqueous phase extraction of pyrolysis oils allows for the removal of the pyrolytic lignin content [16] and yields the so called "sugar fractions" in which up to 80% chemical content of the pyrolysis oils is retained in the form of sugar monomers and oligomers [17]. Although these sugar fractions are largely free from lignin, a suitable upgrading procedure is still highly desirable. For example, direct co- feeding of sugar fractions with methanol, followed by the methanol to hydrocarbon (MTH) process [18] leads to thermal coke formation and catalyst deactivation [16] due to the high monosaccharide and oligosaccharide content of the feed. A desired upgrading procedure converts these saccharides to smaller molecules, preferably aliphatic alcohols, and yields product

* Corresponding author. Tel.: +31 503634232.
** Corresponding author. Tel.: +31 50 3634174.
E-mail addresses: k.barta@rug.nl (K. Barta), h.j.heeres@rug.nl (H.J. Heeres).

http://dx.doi.org/10.1016/j.apcatb.2014.10.065
0926-3373/

mixtures with significantly improved H/C ratios, suitable for direct co-feeding with methanol [19].

Besides processing to hydrocarbons through the MTH processes, mixtures of higher branched and n-alcohols (>C2), directly obtained by upgrading of sugar fractions may be potentially used as fuels or blended with gasoline. Indeed, several studies are focusing on the large scale and cost-effective production of butanol and pentanol isomers, since these alcohols show suitable fuel properties [20–22].

The cost of noble metals usually contained in hydrogenation catalysts is limiting in terms of large-scale application, therefore research should primarily focus on catalyst based on inexpensive and earth-abundant metals [23–26]. Cu-based catalysts have demonstrated unique activity in hydrogenolysis of sugars, sugar alcohols and cellulose [27,28], opening particularly appealing opportunities for catalytic valorization of biomass. Palkovits and co-workers [29] investigated the use of Cu-based catalyst in the hydrogenolysis of cellulose in the aqueous phase, with full conversion of cellulose at 245 °C applying 50 bar H_2. High overall yields of liquid-phase products of up to 95% were obtained, among which 67.4% were C_1–C_3 compounds. Gallezot and co-workers [30] reported the use of a CuO–ZnO catalyst in the hydrogenolysis of sugar alcohols such as sorbitol with 63% selectivity to deoxyhexitols at 180 °C with 130 bar H_2 pressure in the aqueous phase.

Copper doped porous metal oxide (Cu-PMO) was successfully utilized in the full depolymerization and efficient conversion of cellulose and woody biomass in supercritical methanol [31] at 320 °C and 160–220 bar pressure. A mixture of C_2–C_6 aliphatic alcohols and methylated derivatives were reported as the major product when cellulose was used as substrate, and little or no char was formed during this process. Subsequently, Wu et al. [32] reported a series of CuO-based catalysts including CuO–MO_x/Al_2O_3 (M = Ce, Mg, Mn, Ni, Zn) in the reductive disassembly of cellulose to alcohols, among which CuO–ZnO/Al_2O_3 exhibited the highest cellulose conversion of 88% and above 95% C_4–C_7 alcohols content as liquid phase products.

Based on these reports, copper-doped porous metal oxides appear to be ideal candidates for the catalytic upgrading of pyrolysis oils or sugar fractions derived thereof. Here, we report on the realization of this concept, using Cu-PMO catalysts in supercritical methanol and supercritical ethanol. In addition, model compound studies using levoglucosan and D-cellobiose provide insight into the reactivity of these crucial components. We determine the extent of depolymerization and product stability upon upgrading and provide extensive catalyst characterization before and after reaction, as well as leaching and recycling experiments.

2. Experimental

2.1. Materials

Sodium carbonate (≥99.5%), aluminium chloride hexahydrate (99%), magnesium chloride hexahydrate (≥99%) and copper(II) nitrate hemi(pentahydrate) (≥98%), methanol (anhydrous, 99.8%), ethanol (99.8%), 1-propanol (anhydrous, 99.7%), n-butanol (anhydrous, 99.8%), n-pentanol (> 99%), n-hexanol (anhydrous, ≥99%), n-heptanol (98%), di-n-butyl ether(anhydrous, 99.3%) were purchased from Sigma–Aldrich. Levoglucosan and D-cellobiose were purchased from Carbosynth, UK. All chemicals and solvents were used as received. Pyrolysis oils (pine wood) were obtained from BTG (Biomass Technology Group, Enschede, The Netherlands). Sugar fractions were obtained by extraction of pyrolysis oils with water [33,34] following a non-disclosed continuous fractionation procedure of pine derived pyrolysis oils. The obtained sugar fractions (typically 30–40 wt% of the pyrolysis oils) were further treated in a film evaporator to remove water and light organic compounds such as acetic acid, formic acid, methanol, and acetol.

2.2. Catalyst preparation

The catalyst precursor, a copper-doped hydrotalcite, was prepared according to a co-precipitation method described below. A solution containing 0.10 mol $AlCl_3{\cdot}6H_2O$ (24.14 g), 0.06 mol $Cu(NO_3)_2{\cdot}2.5H_2O$ (13.95 g) and 0.24 mol $MgCl_2{\cdot}6H_2O$ (48.80 g) in 0.4 L of deionized water was added to a solution containing 0.10 mol Na_2CO_3 (10.60 g) in 0.5 L of water at 60 °C under vigorous stirring. The pH was maintained between 9 and 10 by addition of small portions of 1 M NaOH solution. The mixture was vigorously stirred at 60 °C for 72 h. After cooling to room temperature, the clear blue solid was filtered and re-suspended in a 2 M solution of Na_2CO_3 (0.3 L) and stirred overnight at 40 °C. The blue solid was filtered and washed with deionized water until chloride-free. After drying at 100 °C for overnight, 29.8 g of the Cu-HTC was isolated. A 10.0 g sample was calcined at 460 °C for 24 h in air to yield 5.6 g of copper doped porous oxide catalyst (Cu-PMO).

2.3. Catalyst characterization

2.3.1. XRD of the HTC precursor and PMO

Powder X-ray analysis was performed on a Bruker XRD diffractometer using Cu Kα radiation and the spectra were recorded in the 2θ angle range of 10–70°.

2.3.2. NH_3-temperature programmed desorption (NH_3-TPD)

NH_3-TPD experiments were carried out in a Micromeritics AutoChem II system equipped with a thermal conductivity detector. The sample was pretreated by heating it up to 500 °C in helium flow (50 mL/min STP) at 10 °C/min. It was cooled to 120 °C at a similar cooling rate, and then exposed to 1 vol.% NH_3/He (25 mL/min STP) for 30 min. Subsequently, a flow of He (25 mL/min STP) was passed through the reactor for 60 min to remove weakly adsorbed NH_3 from the sample surface. After baseline stabilization, the desorption of NH_3 was monitored in the range of 120–1000 °C using a heating rate of 10 °C/min. Acid sites density values are given as arbitrary units due to baseline offset at high temperature. For comparison, a blank omitting the NH_3 adsorption step was performed.

2.3.3. Transmission electron microscopy (TEM)

The images were recorded on a Philips CM12 electron microscope with a slow scan CCD camera at 120 keV. Sample preparation for TEM images was as follows: a small sample of the material was homogenized in a mortar and 1 mg of the fine powder was placed in an Eppendorf vial. A.R. grade EtOH (1 mL) was added and the sample was shaken and sonicated for 10 min. A droplet (ca 2 μL) of the suspension was placed in the middle of a plain carbon coated copper grid (400 mesh). The solvent was allowed to evaporate before imaging.

2.3.4. Inductively coupled plasma-optical emission spectrometry (ICP-OES)

ICP was performed on a PerkinElmer 7000 DV. For the solid samples, ~20 mg was added to an aqueous solution of HNO_3 (8 mL, 65 wt%). Sample destruction was performed in a microwave oven. The sample was heated to 200 °C in 10 min, then held at 200 °C for 15 min. Subsequently, HNO_3 solution (2 wt% in water) was added to a total volume 50 mL. The resulting solution was diluted 10 times with deionized water.

2.3.5. Water content

The water content of sugar fraction was determined using a Karl-Fischer (Metrohm 702 SM Titrino) titration procedure. About 0.01 g

of sample was introduced to an isolated glass chamber containing Hydranal solvent (Riedel de Haen) using a 1 mL syringe. The titration was carried out using Hydranal titrant 5 (Riedel de Haen). Milli-Q water was assumed as 100% pure water standard and used to calibrate the results of titration. All analyses were carried out at least in duplicate and the average value is reported.

2.3.6. Experimental procedures

Catalytic reactions in supercritical methanol and ethanol were carried out in a 100 mL batch autoclave set-up (Parr, max. 350 °C and 350 bar). The reactor was equipped with an electric heater and cooling coil (water) to allow operation at constant temperature. The reactor was heated to the desired temperature with a rate of 10 °C/min. The reaction mixture was stirred with an overhead stirrer with four blades impeller at 1400 rpm. Temperature and pressure were continuously measured in the reactor vessel and monitored by a computer.

2.3.7. Catalytic reactions of levoglucosan and D-cellobiose in supercritical methanol

In a typical experiment the reactor was charged with levoglucosan (1.0 g), or D-cellobiose (1.0 g) followed by 30.0 g of methanol and 1.0 g of Cu-PMO. The reactor was pressurized with N_2 to 100 bar and the pressure was recorded in time to check for leakage. The reactor was subsequently depressurized and flushed 3 times with 20 bar H_2 to remove residual air. The reactor was pressurized with 50 bar H_2 and heated up to 275 °C. After a pre-determined reaction time, the reactor was rapidly cooled down to room temperature. The pressure in the reactor was recorded and the gas phase was sampled using a gas bag. The content of the reactor was transferred to a centrifuge tube, weighed and subsequently centrifuged at 4500 rpm for 30 min. The liquid phase was separated from the catalyst residue by decantation. The spent catalyst was washed twice with methanol (30 mL), and dried in an oven at 100 °C until constant weight.

2.3.8. Representative procedure for catalytic reaction of the sugar fraction in supercritical methanol and ethanol

The reactor was charged with 1.0 g of Cu-PMO and 30.0 g of 5 wt% sugar fraction in methanol. The reactor was sealed and pressurized to 100 bar with N_2 and the pressure was recorded in time to check for leakage. The reactor was depressurized and flushed with 20 bar H_2 to remove residual air. The reactor was subsequently pressurized to 50 bar with H_2. The reactor was heated to 275 °C and then kept at this temperature for the pre-determined reaction time. Work-up was performed as described above. For the catalytic runs in ethanol, 25.0 g of a 15 wt% of sugar fractions in ethanol was applied.

2.3.9. Catalyst recycling in supercritical methanol

After the 1st run, the spent catalyst was collected in the centrifuge tube and washed with 20 mL of methanol, followed by centrifugation at 4500 rpm for 30 min. The solid and liquid were separated and the spent catalyst was washed 3 times using 30 mL of fresh methanol followed by centrifugation and decantation. The spent catalyst was dried in the oven at 100 °C for 12 h and weighed. The same procedure was applied for the 2nd and 3rd run.

2.3.10. Gas chromatography/mass spectrometry (GC–MS)

GC–MS analyses of the liquid phase products were performed on a Hewlett-Packard 5890 gas chromatograph equipped with a quadrupole Hewlett-Packard 6890 MSD selectiver detector and a 30 m × 0.25 mm, i.d. and 0.25 μm film sol–gel capillary column. The injector temperature was set at 250 °C. The oven temperature was kept at 40 °C for 5 min, then increased to 250 °C at a rate of 3 °C/min, and then held at 250 °C for 10 min.

2.3.11. Calibration of mono-alcohols using same carbon number mono-alcohols as standard

Since there are various alcohols (isomers) present in the liquid phase, authentic standards were not available for each separate component. It was assumed that the isomers containing equal carbon numbers have the same relative response factors as their linear counterparts. Thus for calibration, C_2–C_7 n-alcohols were used and di-n-butyl ether was selected as internal standard. Two solutions, A and B, with different concentrations were prepared. Solution A consisted of C_2–C_7 n-alcohols, 1.0 g each. Solution B is composed of 5.5 g of methanol and 0.05 g di-n-butyl ether. Three different standard solutions C1, C2 and C3 were prepared by dilution (in a range of 30–50 times in order to get an average response factor) adding known aliquots of B to A. Solutions C were then injected in GC–MS and an average response factor for each n-alcohol was obtained. For the mixtures obtained after catalytic treatment, 1 wt% of di-n-butyl ether was added and the concentration was calculated according to the peak area and relative response factors.

2.3.12. Silylation method for sugar analysis

The total amount of monosaccharides in the sugar fraction was quantified as follows: carefully dried samples (1–20 mg) were subjected to methanolysis (1 M methanolic HCl, 85 °C, 24 h with 100–500 nmol of D-mannitol internal as standard). The resulting mixture was neutralized and washed twice with dry methanol. The supernatants were then evaporated to dryness under reduced pressure (100 mbar at 35–37 °C). The residue was trimethylsilylated (1:1:5 hexamethyldisilazane–trimethylchlorosilane–pyridine) for 30 min. The clear solution was then injected on a GC/MS equipped with a Restek Rxi®-5Sil MS column and FID detector. The oven was heated from 140 to 240 °C with a rate of 4 °C/min.

Levoglucosan in the sugar fraction was quantified as follows: carefully dried sugar fraction (1–20 mg with 100–500 nmol of D-mannitol as internal standard) was directly trimethylsilylated (1:1:5 hexamethyldisilazane–trimethylchlorosilane–pyridine) for 30 min. The clear solution was then injected on a GC/MS equipped with a Restek Rxi®-5Sil MS column and FID detector with temperature programme from 140 to 240 °C with a rate of 4 °C/min. The total peak area of each monosaccharide was divided by the peak area of internal standard D-mannitol to obtain the response factor (RF) of each monosaccharide according to the formula:

$$RF_i = \frac{n_i}{n_{is}} \times \frac{A_{is}}{A_i}$$

where RF_i is the response factor (RF) of monosaccharide i, n_i and n_{is} are the amount of monosaccharides i and the internal standard (mol), A_i and A_{is} are the peak areas of the monosaccharide i and the internal standard.

2.3.13. Two-dimensional gas chromatography (2D-GC)

2D-GC analyses of the products from the reaction of a 15 wt% of sugar fractions in ethanol was performed on a Trace 2D-GC system from Interscience equipped with a cryogenic trap and two capillary columns connected to a 148 cm × 0.1 mm, i.d. and 0.1 μm film Restek 1701 column. A flame ionization detector (FID) was used. A dual-jet modulator was applied using CO_2 to trap the samples. The lowest possible operating temperature for the cold trap was 60 °C. Helium was used as the carrier gas (flow rate 0.6 mL/min). The injector temperature was kept at 60 °C for 5 min and then increased to 250 °C at a rate of 3 °C/min. The pressure was set at 0.7 bar. The modulation time was 6 s.

2.4. Gel permeation chromatography (GPC)

The liquid phase product obtained after catalytic treatment was evaporated at 40 °C, 100 mbar for 20 min to remove the solvent.

0.05 g of the organic residue as well as 0.05 g of sugar fraction was dissolved in 5 mL of THF (10 mg/mL) and 2 drops of toluene were added as molecular weight marker. The resulting suspension was filtered (pore size 0.2 μm) before injection. An Agilent HPLC 1100 system equipped with a refractive index detector and three columns in series (mixed type E, length 300 mm, i.d. 7.5 mm) were used. Polystyrene was used as a calibration standard was used.

2.5. Thermogravimetric analysis (TGA)

TGA data of sugar fractions and the evaporated products from sugar fractions were determined using a TGA 7 from Perkin-Elmer. The samples were heated in a nitrogen atmosphere with a heating rate 10 °C/min and a temperature range between 20 and 900 °C.

2.6. N_2O chemisorption

Copper surface area (MSA) and dispersion (D_{Cu}) values were obtained by "single-pulse" N_2O-titration measurements at 363 K. The samples were reduced at 573 K in flowing H_2 (100 stp mL/min) for 1 h prior to measurement, then "flushed" at 583 K in nitrogen carrier flow (15 min) and further cooled down at 363 K. MSA and D_{Cu} values were calculated assuming a Cu:N_2O = 2:1 titration stoichiometry, according to the reaction $2Cu + N_2O \rightarrow Cu_2O + N_2$, and a surface atomic density of 1.46×10^{19} Cu_{at}/m^2, respectively [35]. The Cu average particle size (d_{Cu}) was calculated from the conventional formula: d_{Cu} (nm) = $104/D_{Cu}$ (%), assuming a spherical shape for the copper particles [35].

3. Results and discussion

3.1. Experimental studies on model sugars in supercritical methanol over Cu-PMO

The main bottleneck of cleanly converting sugar fractions of pyrolysis oils is the presence of higher and lower molecular weight sugars as well as levoglucosan [36]. Feeding of sugars directly in processes operating with zeolite catalysts, leads to significant amounts (30–70%) of coke formation due to low H_{eff}/C ratios [37–39]. Anhydrosugars, e.g. levoglucosan, and furans were assumed as the primary products from glucose in zeolite process, which ultimately decompose to unsaturated coke [39]. So conversion of sugar monomers and oligomers as well as levoglucosan from sugar fraction of pyrolysis oils is an efficient way to suppress excessive coke formation.

In order to gain insight into the reactivity of the sugar fraction, we have performed catalytic runs using levoglucosan and D-cellobiose in supercritical methanol, using Cu-PMO, under selected reaction conditions. The same catalyst was also successfully applied by our group in the reduction of 5-HMF to DMF [40]. Levoglucosan is the most prominent component (28.0 wt%) of the sugar fraction used in this study and D-cellobiose is a representative molecule for sugar oligomers. First, the reactivity of levoglucosan was assessed (Fig. 1, left). Catalytic runs were performed in supercritical methanol using a standard Parr reactor setup. Initial screening was conducted at 250 °C with no significant substrate conversion. At higher reaction temperatures (300 °C), methanol reforming over Cu-PMO led to increase in pressure and did not allow for monitoring product composition over longer reaction times. Thus, 275 °C was selected as suitable reaction temperature and relevant changes in the composition of product mixtures could be monitored over 8 h, in single batch runs. The liquid phase products were analyzed by GC–MS, which allowed for identification and quantification of all main components. The evaluation of main groups of components over time is depicted in Fig. 1 (left) and the results are summarized in Table 1. For more details, see supporting information, Table S1.

Table 1
Classes of compounds obtained using levoglucosan at various reaction times in supercritical methanol.[a]

Products	GC selectivity (%)			
	2 h	4 h	6 h	8 h
Alcohols	56	68	71	77
Esters	13	11	10	9
Diols	15	13	10	3
Ethers	12	3	3	3
Ketones and aldehydes	2	0	0	0
Furanics and pyranics	2	5	6	7

[a] 1.0 g levoglucosan, 1.0 g catalyst, 275 °C, 50 bar H_2.

In these catalytic runs, clean and full conversion of levoglucosan was observed already after 2 h and the liquid phase consisted of various low boiling products that generally fall into the following chemical categories: aliphatic mono alcohols, diols, ethers, esters, aliphatic ketones and aldehydes, furanics and pyranics. Among these products, C_2–C_7 mono-alcohols were largely prevalent in the product mixture. Their selectivity gradually increased from 56% at 2 h to 68% and 71% at 4 and 6 h, respectively. Mono alcohol selectivity further increased to 77% in 8 h, mainly due to the conversion of diols. The quantity of diols and ethers in the product mixture peaked at 2 h, representing 15% and 12% selectivity, respectively. Carbonyl containing compounds were only present in small quantities at 2 h, after which they were fully reduced. In contrast, the amount of furanics and pyranics gradually increased from 2% to 7% albeit their amount stayed relatively low.

Similarly, the amount of esters was relatively constant in time (between 12 and 9%), suggesting that they do not get further converted under these reaction conditions. Esters and ethers were likely formed through reaction of free —OH groups with the solvent methanol, but their selectivity did not exceed 12% after 8 h (see also Table S1).

This suggests, that levoglucosan undergoes slightly different conversion pathways compared to D-cellobiose, which keep the cyclic structure of the substrate initially intact. Under acidic conditions, levoglucosan has been shown to undergo rapid solvolysis and ring opening in methanol to form methyl α-D-glucopyranoside (MGP) [41], however the catalyst used in this study does not comprise acidic sites, as determined by NH_3-TPD measurement. (supporting information, Fig. S1, Table S3). If levoglucosan would first be converted to a monosaccharide, the product profiles would be very similar to those obtained with D-cellobiose. However, D-cellobiose displays a significant amount of diols (42%) after 2 h reaction time as shown in Table 2 and Fig. 1 (right). These diols undergo further deoxygenation to mono alcohols as shown by the gradual decrease in selectivity from 28, 11, and 9 in 4, 6 and 8 h respectively. Accordingly, the mono-alcohol selectivity increases to 54, 64 and 67 at the same reaction times. Interestingly, in contrast to the runs with levoglucosan, ether selectivity increases with

Table 2
Classes of compounds obtained using D-cellobiose in supercritical methanol.[a]

Products	GC selectivity (%)			
	2 h	4 h	6 h	8 h
Alcohols	44	54	64	67
Esters	7	12	15	11
Diols	42	28	11	9
Ethers	5	5	9	10
Ketones and aldehydes	1	0	<1	<1
Furanics and pyranics	1	1	1	2

[a] 1.0 g D-cellobiose, 1.0 g catalyst, 275 °C, 50 bar H_2.

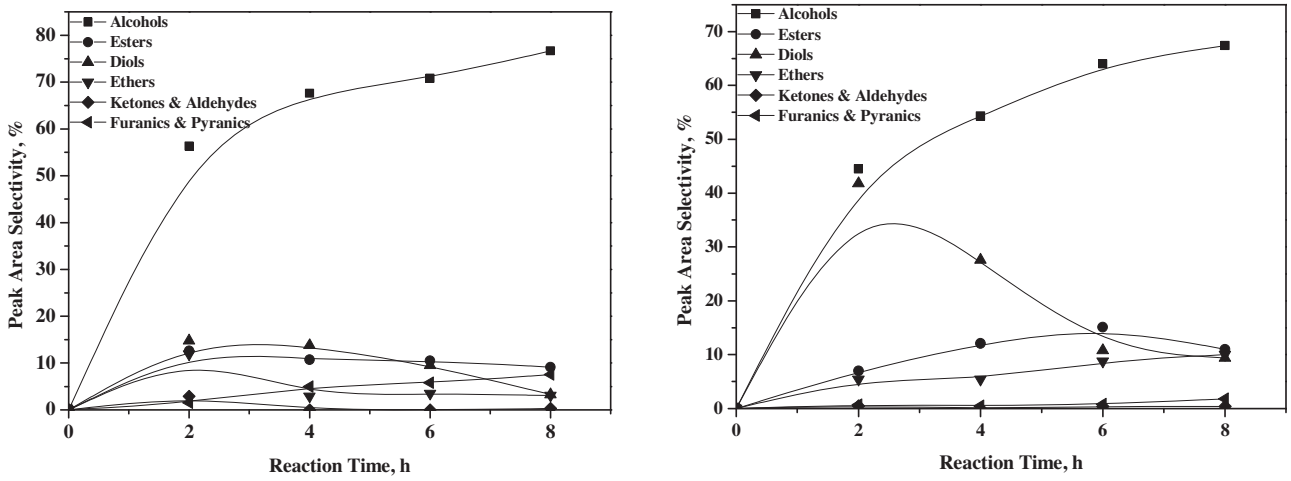

Fig. 1. Products from levoglucosan (left) and D-cellobiose (right) in supercritical methanol over Cu-PMO.

time, reaching 10% at 8 h, due to the formation of methyl ether species of several abundant diols (e.g. ethylene glycol is converted into 2-methoxyethanol). The amount of esters remains relatively constant over time, between 7 and 15%. In general, compared to the runs with levoglucosan, the solvent engages in reactions with D-cellobiose to higher extent due the larger presence of diols, giving up to 21% methylated compounds after 8 h.

In general, these product formation profiles are consistent with reports describing the reactivity of glucose, cellulose or sugar derived polyols over supported metal catalysts and basic Cu catalyst under hydrogenation conditions [27,29,30]. These studies demonstrate the existence of various pathways, including retro-aldol condensations, hydrogenations and deoxygenations and chain shortening by C—C bond cleavage, generally yielding either hexitols (under milder conditions) or diols and short chain mono-alcohols as main products under harsher reaction conditions [31].

Overall these results suggest, that sugar fractions derived from pyrolysis oils can be efficiently converted, as both model components levoglucosan as well as sugars are reactive in this system. Notably, for both D-cellobiose and levoglucosan no char formation was observed.

3.2. Studies using sugar fractions

Sugar fractions obtained by aqueous extraction of pyrolysis oils, are complex mixtures of organics (e.g. acids, aldehydes, ketones) and sugar monomers and oligomers originating from the decomposition of cellulose and hemicellulose during the pyrolysis process. In addition, they contain water (14.5 wt%) albeit not as extensively as pyrolysis oils (up to 30 wt%). The product mixtures after catalytic treatment also consist of multiple chemical components. To deal with this analytical challenge, we have identified groups of components in the starting material as well as in the product stream. This allows for describing the overall chemical composition and the nature of chemical changes taking place during the upgrading procedure.

The non-volatile sugars were analyzed by a silylation method and the results are shown in Table 3. According to these measurements, monosaccharides represent the main components of sugar fractions. The monosaccharides identified include arabinose (1.31 wt%, dry basis), xylose (1.99 wt%, dry basis), mannose (13.15 wt %, dry basis), galactose (5.40 wt%, dry basis) and glucose (46.32 wt%, dry basis). The water content in the sugar fraction is 14.5 wt%. The amount of levoglucosan was 28.0%, as separately assessed by direct silylation of the sugar fraction and subsequent GC analysis.

Table 3
Sugar analysis by silylation of sugar fractions from pyrolysis oils.

Sugar type	wt%, dry base
Arabinose	1.3
Xylose	2.0
Mannose	13.2
Galactose	5.4
Glucose	46.3
Total sugars	68.2
Water content	14.5

The volatile fraction of sugar fractions was determined by direct GC–MS/FID measurement. It was found to consists 5% of acids (mainly acetic acid), 41% of ketones and aldehydes (mainly hydroxylaldehyde and hydroxylacetone), 44% levoglucosan, 8% phenolics and 2% furanics as shown in Fig. 2 and Table 4 (for details of the composition see supporting information, Table S4).

Catalytic runs were performed in supercritical methanol using the same reaction conditions adopted for the model compound studies (1.0 g of Cu-PMO, 30.0 g of 5 wt% sugar fraction, 275 °C). After 8 h, a colourless solution was obtained, which was analyzed by GC–MS. The overall composition of the product mixture is shown in

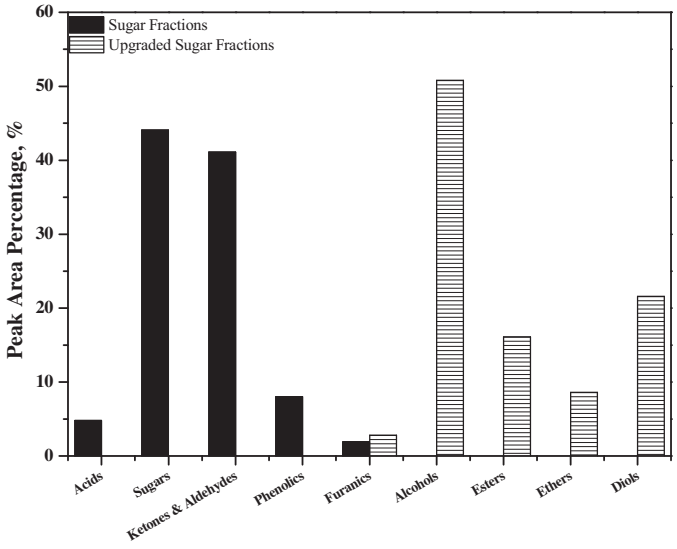

Fig. 2. Different classes of compounds present in the sugar fraction and upgraded sugar fraction in scMeOH over Cu-PMO, composition determined by GC–MS-FID.

Table 4
Volatiles in the sugar fraction and upgraded products.[a]

Sugar fractions	Area percentage (%)	Upgraded sugar fraction	Area percentage (%)
Acids	5	Alcohols	51
Ketones and aldehydes	41	Esters	16
Sugars	44	Diols	22
Phenolics	8	Ethers	8
Furanics	2	Furanics	3

[a] These percentages are relative numbers based on total area percentages determined by GC–MS-FID.

Fig. 2 while the detailed composition of the product mixture is given in the supporting information, Table S5. The analysis indicates very similar product distribution to the model compound studies with cellobiose, albeit with slightly lower mono alcohol (51%) and higher diol (22%) selectivity. Other compounds include 16% of esters, 8% of ethers and 3% of furanics. The latter represent the only stable aromatic products since quite reactive phenolics are mainly overreduced to cyclohexanol derivatives. The yield of obtained product alcohols was additionally confirmed by a calibration protocol as described in supporting information, Table S6.

A change in composition of sugar fractions upon upgrading is shown in Table 4 and Fig. 2. The comparison shows, that the chemical components in the sugar fraction underwent important changes, including reduction, etherification, esterification and overall deoxygenation, resulting in product mixtures with improved H/C rations, thus significantly better suited for direct co-feeding into MTH processes.

For industrial scale applications, upgrading of sugar fractions of much higher concentration is desired. Thus further effort concentrated on converting 15 wt% sugar fractions. Due to the high concentration of the feed however, we have applied ethanol as solvent at 300 °C for 8 h. This allowed for more precise control of reaction pressure, which was achieved by addition of 50 bar H_2 as no solvent reforming took place in this case. Analysis of the product mixture was carried out using 2D-GC as shown in Fig. 3. Gratifyingly, three distinct areas, attributable to aliphatic mono-alcohols, diols and esters were seen on the 2D-GC trace and confirmed by spiking with pure authentic standards. These main groups of compounds are in agreement with the product composition of the reaction of 5% sugar fraction in supercritical methanol. Notably, even at the present significantly higher substrate loading (3.95 g sugar fraction and 1.00 g catalyst) the sugar fraction was extensively transformed to ethanol soluble small molecules, while 0.23 g (5.8 wt%) insoluble residue was detected by weighing the solids after reaction. Addition of aqueous HNO_3 did not afford a clear solution (Fig. S2 in supporting information), likely due to a small amount of unreacted organics. However, no insoluble solid was accumulated in the sample obtained after reaction in scMeOH; here only 0.86 g solid could be recovered and no extensive precipitate was observed after dissolving in HNO_3 (Fig. S2 in supporting information).

The catalytic valorization of pyrolysis oils and its lower and higher boiling fractions using supported Pt or Pd noble metal catalysts on various supports including SiO_2, Al_2O_3, MgO, ZnO, ZrO_2 in supercritical methanol or ethanol has been reported [42–44]. Generally, low boiling fractions (volatiles) can be to a large extent upgraded to esters [42] but for the distillation residues, which contain larger molecule such as sugars and lignin fractions, significant char formation was observed [43]. In contrast, our methodology uses an inexpensive catalyst (Cu-PMO) and the whole of the sugar fraction, including larger sugar molecules were cleanly upgraded to mixtures of small molecules, mainly shorter chain aliphatic alcohols with no or low amount of coke deposition.

In general, the groups of chemical compounds obtained after catalytic valorization in supercritical methanol over Cu-PMO are expected to display a much better cracking performance compared to mother sugar fractions from pyrolysis oils. Branched and linear aliphatic alcohols constitute the predominant components of the product mixture, and are expected to be highly suitable for the production of aliphatic and aromatic hydrocarbons thorough co-feeding into zeolite processes [45]. Their dehydration to the corresponding olefins readily occurs at ~200 °C. Ketones, e.g. hydroxylacetone and acetone, which are still present in the sugar fraction in higher quantities, are less suitable for direct co-feeding [46]. However, in our system, these components are fully converted to mono-alcohols. Compared to ketones, aldehydes are even more challenging substrates for HZSM-5 procedures. Reasons for low

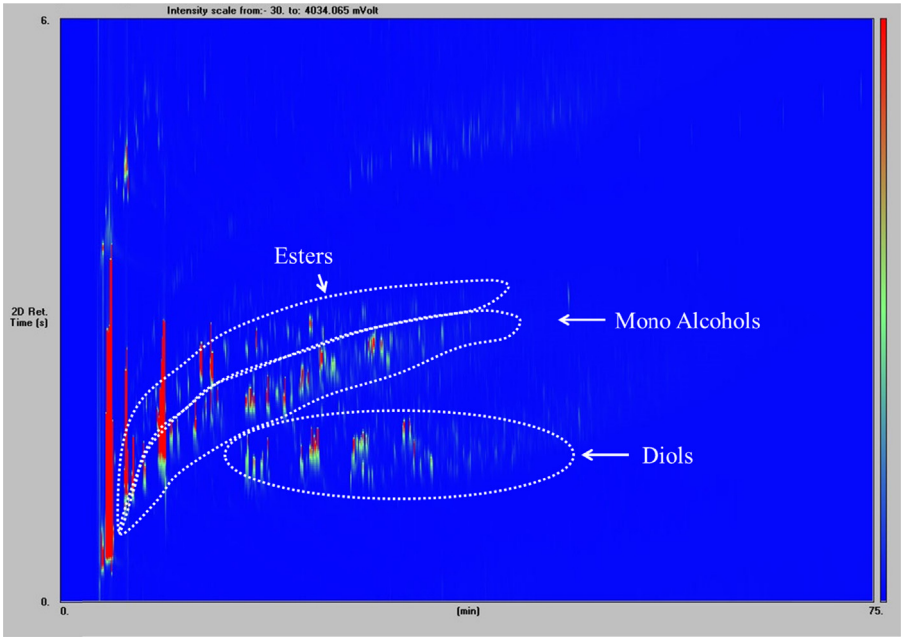

Fig. 3. 2D-GC spectrum a representative upgraded product using 15 wt% solution of a sugar fraction in supercritical ethanol over Cu-PMO.

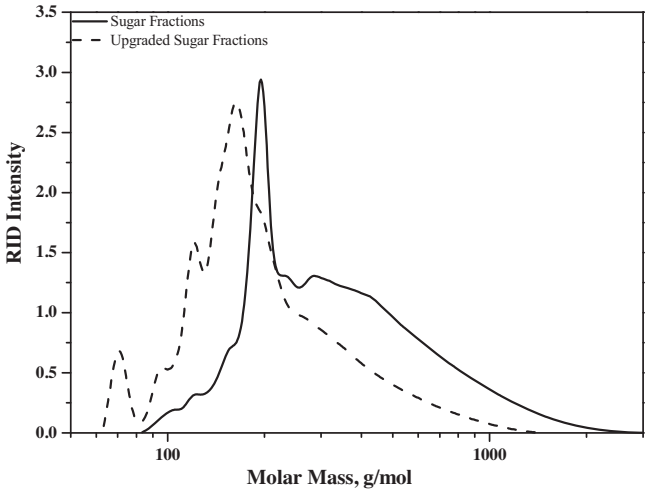

Fig. 4. Comparison of the molecular weight distribution of sugar and upgraded sugar fractions determined by GPC chromatography.

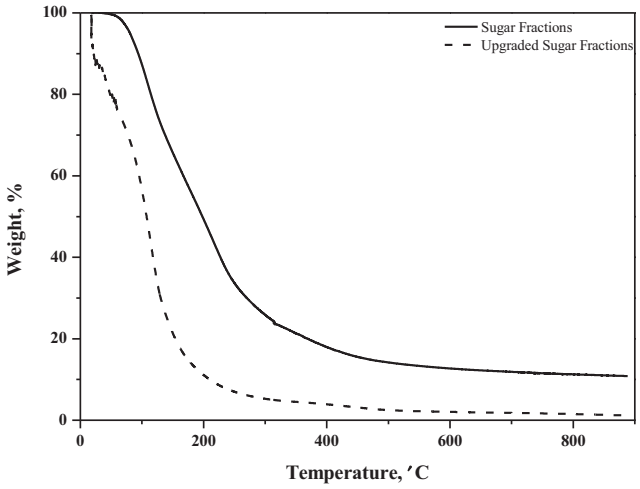

Fig. 5. Comparison of TGA curves of sugar fraction and upgraded sugar fraction.

compatibility are side reactions such as the formation of trimethyltrioxane as well as thermal degradation [46]. During upgrading over Cu-PMO, acetaldehyde is converted to methyl acetate and ethanol [47]. A very interesting group of products obtained upon upgrading are esters, presumably from esterification of carboxylic acids present in the sugar fractions with methanol [48] and from sugar oligomers in supercritical methanol [32]. It has been reported that esters favour oxygen removal through decarbonylation over dehydration, which preserves the hydrogen content of the hydrocarbon product mixture [19].

Clearly, the products after catalytic valorization in supercritical methanol or ethanol over Cu-PMO are much more suitable for co-feeding in MTH process compared to sugar fractions from pyrolysis oils.

3.3. Depolymerization and thermal stability of the upgraded sugar fractions

Depolymerization of the residual oligosaccharides contained in sugar fractions is another crucial factor for co-feeding in methanol for zeolite processes due to the microporosity of the catalyst [49]. To prove depolymerization of oligosaccharides in our system, we performed GPC analysis of both the sugar fraction as well as the upgraded products. A comparison of the GPC traces is shown in Fig. 4. The majority of the components from the parent sugar fractions are in higher molecular range and long tail is observed. Relevant changes in the molecular weight distribution of the sugar fractions were detected upon catalytic treatment: the area of the broad signal belonging to the higher molecular weight range decreased, and the average molecular weight shifted from 407.2 g/mol for the starting material to 233.5 g/mol for the upgraded product. In the GPC trace of the product, a sharp peak in low molecular range (<200 g/mol) and a broad peak in higher molecular range (>200 g/mol) can be seen. We would like to point out that at lower molecular weight ranges, there is a variation in the precision of a GPC measurement. In fact, according to calibration and GC-FID analysis the product mixture predominantly consists of small molecules. Nonetheless, the comparison of the GPC traces shows significant changes in terms of molecular weight distribution.

The use of supercritical alcohol media is especially suited to prevent repolymerization reactions, and have significant effect on the stabilization of sugar fractions. The esterification and acetalization of the sugar components prevent further chain growth, as acetals serve as protecting groups for aldehydes and ketones [50]. The thermal stability of the upgraded products is an important characteristic prior to co-feeding procedures. This value is a measure for the coking tendency of the product; a higher value indicates a lower thermal stability. Thermal stability was determined by TGA experiments and involves heating up a sample to elevated temperatures (900 °C) and measuring relevant weight changes of the sample while reaching the final temperature. The comparison of the TGA results of sugar fractions and products after 8 h reaction in supercritical methanol are given in Fig. 5.

The TGA curve indicates a 94.8% weight loss of upgraded product at ~300 °C, compared to 74.2% for the sugar fraction. This is consistent with the observed depolymerization of oligosaccharides in the sugar fractions, and the change of composition towards more volatile fractions in the upgraded product. At 900 °C, the solid residue for the upgraded sugars is 1.1%, while 10.8% was measured for the parent sugar fractions. This result clearly shows that the upgraded product is much more stable and more suitable for direct co feeding.

3.4. Catalyst characterization

The XRD patterns of the synthesized hydrotalcite sample (Cu-HTC) and calcined sample (Cu-PMO) are shown in Fig. S3. The hydrotalcite sample showed highly ordered crystalline structures with diffraction patterns consistent with literature data for hydrotalcite-like materials [51,52]. The characteristic doublet at 60°, which is representative for a double-layered structure, is distinctly visible [51]. After calcination, a porous near-amorphous material with a BET surface area of 197 m^2/g was obtained. This material was identified by the lack of any characteristic HTC reflections and the appearance of weak MgO and CuO reflections [28,52]. The empirical composition of the obtained Cu-PMO, determined by elemental analysis [$Cu_{0.59}Mg_{2.34}Al_{1.00}$] (see also Table 7, entry 1) is in very good agreement with the expected theoretical values [$Cu_{0.60}Mg_{2.40}Al_{1.00}$].

3.5. Catalyst characterization by transmission electron microscopy (TEM)

The catalyst before and after reaction was analyzed by TEM as shown in Fig. 6 and 7. In the fresh catalysts, patchy objects were seen, consisting of multiple aggregated fine sheets. The aggregates were usually bigger than 100 nm × 100 nm. The sheets were almost

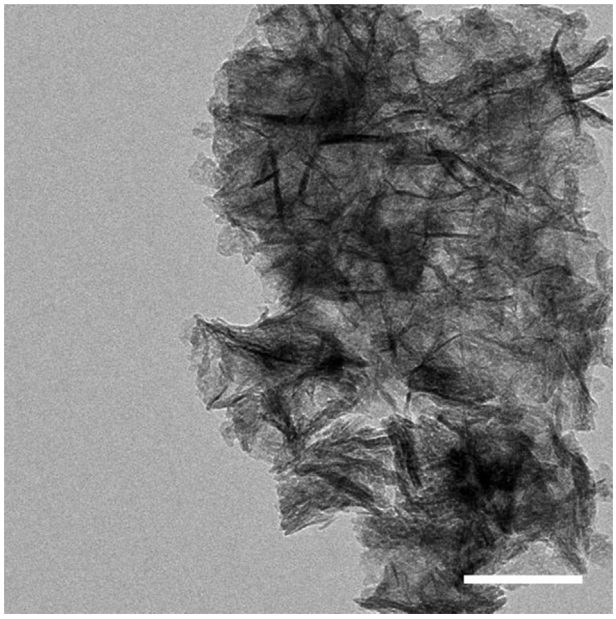

Fig. 6. TEM image of Cu-PMO before reaction. Scale bar is 50 nm.

Table 5
Results of N_2O titration measurements.

Sample	MSA (m^2_{Cu}/g_{cat})	D_{Cu} (%)	d_{Cu} (nm)
Fresh Cu-PMO	5.8	5.5	19
Spent Cu-PMO (MeOH)	2.4	2.3	45
Spent Cu-PMO (EtOH)	1.7	2.4	43

transparent, which suggests that they consist of a material of low density (probably Mg and Al oxides).

The spent catalyst after the reaction in supercritical ethanol and methanol was also imaged. A comparison between the TEM images is shown in Fig. 7. In both samples patchy objects, consisting of multiple aggregated fine sheets with similar morphology to those in Cu-PMO were seen. The unchanged morphology of the sheets suggests that the reaction conditions do not influence significantly the Mg and Al oxide sheets.

Additionally, in both samples, a large number of dense nanoparticles (probably CuNPs) were detected, attached to the surface of the sheets. An apparent difference between the two samples after reaction is in the size and dispersity of the nanoparticles. In the sample obtained after reaction in supercritical ethanol (shown in Fig. 7, A), the nanoparticles are polydisperse, with typical sizes ranging from 5 nm to 40 nm.

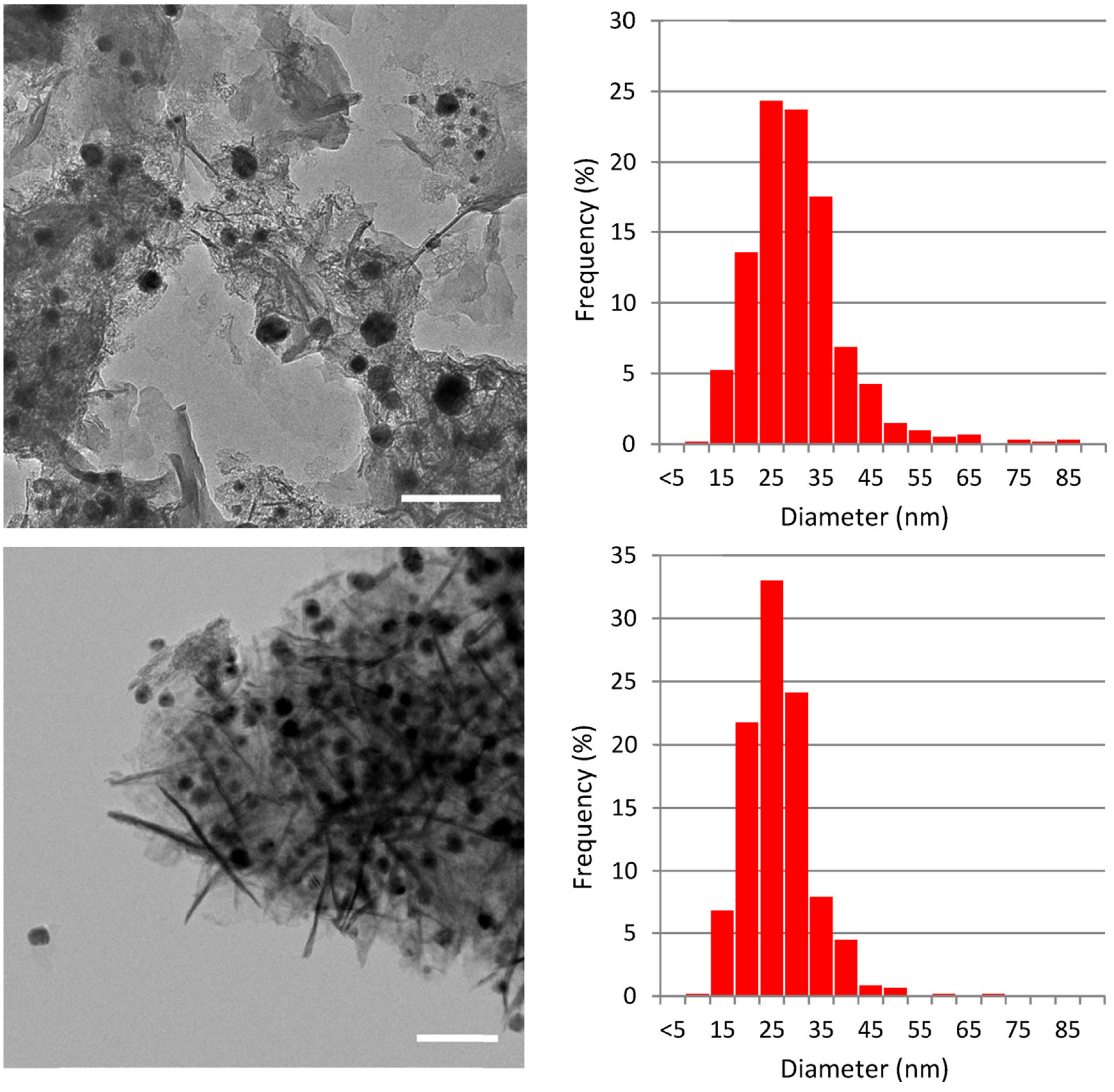

Fig. 7. TEM images of spent catalyst from reactions in scEtOH (top) and scMeOH (bottom), and the corresponding size distribution histograms. Scale bars are 50 nm.

Table 6
The composition of liquid products obtained in recycling experiments using Cu-PMO in scMeOH.

Run	Alcohols, peak area, %	Esters, peak area, %	Ethers, peak area, %	Furanics, peak area, %	Diols, peak area, %
1st	45	24	4	6	21
2nd	31	21	5	11	32
3rd	16	46	2	16	20

In spent catalyst from scMeOH (Fig. 7, B), the nanoparticles are more monodisperse, with typical sizes of 7–15 nm (>80% of the particles). This difference is highlighted in the size distribution histograms in Fig. 7 (see Table S7 in supporting information for more details) and can be attributed to the different operational temperature (275 °C in scMeOH vs. 300 °C in scEtOH) as higher temperatures promote aggregation of copper particles due to surface migration processes [53]. It has been shown, that magnesium oxide stabilizes highly dispersed copper nanoparticles in mixed oxide catalysts obtained from double-layered hydrotalcite structures [54], thus these findings correlate with the extent of magnesium leaching determined for both samples which was almost none for 275 °C in scMeOH and significant for 300 °C in scEtOH (see below in Table 7).

3.6. Copper dispersion measurements

Copper surface area (MSA), metal dispersion (D_{Cu}) and crystallite size (d_{Cu}) values were obtained by N_2O pulse chemisorption and the results are summarized in Table 5. The fresh catalyst displays the highest value of copper surface area, which is in agreement with a better dispersion of nanosized copper crystallites in the initially highly porous material with respect to both spent catalysts. The total metal surface area decreases from 5.8 m^2/g in the Cu-PMO to 2.4 m^2/g for the spent catalyst in scMeOH and further decreases to 1.7 m^2/g clearly due to coalescence of copper particles, as already observed in TEM measurements. Accordingly, copper dispersion is approximately reduced to half respect to the original value (5.5%) after both runs in methanol and ethanol 2.3% and 2.4%, respectively), while the average particles diameter (assuming a spherical shape) seems to consequently double after reaction. The calculated surface copper parameters, especially the dispersion and average particle size, seem to be very comparable after reaction in both alcohols. Particularly, average particle size values differ by less than 20 nm respect to those derived statistically by TEM measurements; however, overrestimation of average particle size by N_2O titration method is commonly observed. Moreover, the fact that the fresh catalyst contains CuO respect to the more dense Cu^0 nanoparticulates of the spent catalysts might explain why we did not observe any visible copper oxide nanoparticle in the Cu-PMO.

3.7. Catalyst recycling and leaching

The stability of Cu-PMO catalyst for catalytic valorization of sugar fractions in supercritical methanol was evaluated in 3 consecutive runs using 1.0 g catalyst, 1.5 g sugar fraction and 28.5 g of methanol at 275 °C for 8 h and the products distribution measured by GC–MS/FID is shown in Fig. 8 and Table 6. For the 1st run, the product mixture consisted of 45% of mono alcohols, 21% of diols and 24% of esters, and slightly less ethers and furanics were also present. These values are consistent with the results shown in Table 4 and Fig. 2. For the 2nd run, a decrease in mono alcohols from 45% to 31% was observed and diols increased from 21% to 32%. The amount of ethers stayed relatively constant and the amount of furanics markedly increased from 6% to 11%. In the 3rd run, mono alcohols formation decreased to 16% and esters 46% were the dominant product. The above results show, that the catalyst activity

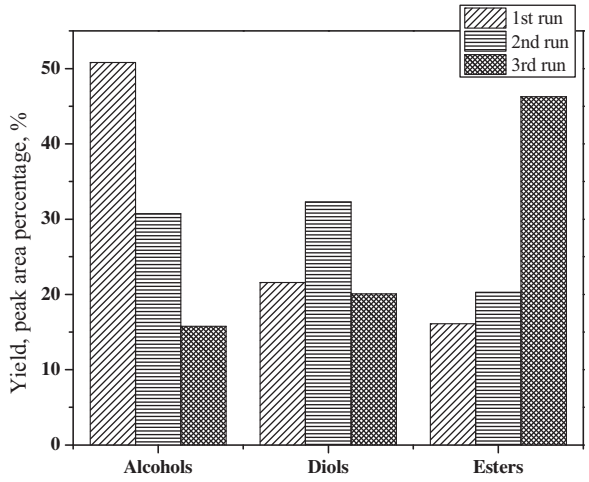

Fig. 8. Classes of compounds obtained in recycling experiments using Cu-PMO in scMeOH.

Table 7
Elemental analysis of fresh and Cu-PMO and after use in scMeOH and scEtOH.

Entry	Sample	Al (wt%)	Cu (wt%)	Mg (wt%)
1	Fresh Cu-PMO	11.7	16.3	24.6
2	Spent Cu-PMO (MeOH)	11.6	16.2	24.0
3	Spent Cu-PMO (EtOH)	9.0	12.6	17.4

changes within 3 cycles, giving rise in product mixtures of varied composition.

Elemental analysis of the fresh catalyst and catalyst residues from both supercritical methanol and ethanol reactions was carried out to determine any leaching in the present cases. Fresh Cu-PMO and the spent catalyst from the experiments in scMeOH and scEtOH were subjected to ICP elemental analysis. The results are compared in Table 7. These experiments show, that loss of active metal content is minimal in the case of supercritical methanol and low substrate loading. However when utilizing much more concentrated sugar fraction solutions which contains 2.3 g water per gram of magnesium, while keeping the same low catalyst amount, leaching of the magnesium content is up to 6.6%, thus more significant.

These results indicate, that although the catalyst is highly suitable for upgrading of sugar fractions, stability needs to be enhanced in order to enable continuous flow operation. The Cu-PMO was successfully utilized and could be recycled multiple times using a variety of biomass sources without any leaching. However, in those studies generally water-free conditions were utilized [28,31,52]. Thus, we believe the loss of activity in the present case is likely due to the up to 15% water content still present in the sugar fraction as well as higher acid content.

4. Conclusions

In conclusion, we have developed an upgrading procedure for sugar fractions obtained from pyrolysis oils using earth abundant catalyst in supercritical ethanol and methanol. The advantage of the reported methodology is, that it leads to highly efficient conversion of the complex set of substrates present in the sugar fraction with

no- or low amount of coke formation. We have identified the composition of the product mixtures using a variety of techniques and described the nature of chemical transformations taking place during these upgrading procedures. The product mixtures obtained are largely aliphatic mono-alcohols, suitable for potential application in co-feeding to MTH processes. Alternatively, the obtained distinct groups of compounds can be further fractionated by distillation. In addition, clean mixtures of linear and branched aliphatic alcohols might be isolated and used as liquid fuel additives with superior performance compared to bioethanol. Further efforts concentrate on improving catalyst stability in order to enable upscaling and continuous flow operation.

Acknowledgments

Financial support from Agentschap NL (Groene aardolie via pyrolyse, GAP) is gratefully acknowledged. We thank R. M. Abdilla (Department of Chemical Engineering, University of Groningen, The Netherlands) for sugar analysis, Dr. F. Frusteri and Dr. G. Bonura (CNR-ITAE, Institute for Advanced Energy Technologies "Nicola Giordano", Messina, Italy) for N2O chemisorption experiments, H. van derVelde (Stratingh Institute for Chemistry, University of Groningen, The Netherlands) for performing the elemental analyses and ICP-OES test, H.Heeres (BTG,Biomass Technology Group, The Netherlands) for the preparation of sugar fractions, M. J. Ortiz Iniesta (Department of Chemical Engineering, University of Groningen, The Netherlands) for the measurement of NH3-TPD and G. O. R. Alberda van Ekenstein (Department of Polymer Chemistry, Zernike Institute for Advanced Materials, University of Groningen, The Netherlands) for TGA analysis. We also thank J. H. Marsman, L. Rohrbach, E. Wilbers, M. de Vries and A. Appeldoorn for technical support.

Appendix A. Supplementary data

Supplementary data associated with this article can be found, in the online version, at http://dx.doi.org/10.1016/j.apcatb.2014.10.065.

References

[1] G.W. Huber, S. Iborra, A. Corma, Chem. Rev. 106 (2006) 4044–4098.
[2] A. Corma, S. Iborra, A. Velty, Chem. Rev. 107 (2007) 2411–2502.
[3] J.N. Chheda, G.W. Huber, J.A. Dumesic, Angew. Chem. Int. Ed. 46 (2007) 7164–7183.
[4] M. Stöcker, Angew. Chem. Int. Ed. 47 (2008) 9200–9211.
[5] M. Besson, P. Gallezot, C. Pinel, Chem. Rev. 114 (2013) 1827–1870.
[6] R. Venderbosch, A. Ardiyanti, J. Wildschut, A. Oasmaa, H. Heeres, J. Chem. Technol. Biotechnol. 85 (2010) 674–686.
[7] A. Oasmaa, D.C. Elliott, J. Korhonen, Energy Fuels 24 (2010) 6548–6554.
[8] D.C. Elliott, Energy Fuels 21 (2007) 1792–1815.
[9] H. Wang, J. Male, Y. Wang, ACS Catal. 3 (2013) 1047–1070.
[10] A.H. Zacher, M.V. Olarte, D.M. Santosa, D.C. Elliott, S.B. Jones, Green Chem. 16 (2014) 491–515.
[11] J. Wildschut, F.H. Mahfud, R.H. Venderbosch, H.J. Heeres, Ind. Eng. Chem. Res. 48 (2009) 10324–10334.
[12] J. Wildschut, I. Melian-Cabrera, H. Heeres, Appl. Catal. B: Environ. 99 (2010) 298–306.
[13] A. Ardiyanti, A. Gutierrez, M. Honkela, A. Krause, H. Heeres, Appl. Catal. A: Gen. 407 (2011) 56–66.
[14] K. Bryden, G. Weatherbee, E.T. Habib, Catalagram 113 (Spring 2013) (2013) 3–21.
[15] F. de Miguel Mercader, M. Groeneveld, S. Kersten, N. Way, C. Schaverien, J. Hogendoorn, Appl. Catal. B: Environ. 96 (2010) 57–66.
[16] A. Gayubo, B. Valle, A. Aguayo, M. Olazar, J. Bilbao, J. Chem. Technol. Biotechnol. 85 (2010) 132–144.
[17] A. Oasmaa, E. Kuoppala, A. Ardiyanti, R. Venderbosch, H. Heeres, Energy Fuels 24 (2010) 5264–5272.
[18] U. Olsbye, S. Svelle, M. Bjørgen, P. Beato, T.V. Janssens, F. Joensen, S. Bordiga, K.P. Lillerud, Angew. Chem. Int. Ed. 51 (2012) 5810–5831.
[19] U.V. Mentzel, M.S. Holm, Appl. Catal. A: Gen. 396 (2011) 59–67.
[20] J.S. Lamoureaux, T.H. Fleisch, US8641788, 2011.
[21] K.L. Jones Prather, H.-C. Tseng, US2012/036524, 2011.
[22] G.R. Dowson, M.F. Haddow, J. Lee, R.L. Wingad, D.F. Wass, Angew. Chem. Int. Ed. 125 (2013) 9175–9178.
[23] A. Ardiyanti, S. Khromova, R. Venderbosch, V. Yakovlev, H. Heeres, Appl. Catal. B: Environ. 117 (2012) 105–117.
[24] A. Ardiyanti, S. Khromova, R. Venderbosch, V. Yakovlev, I. Melián-Cabrera, H. Heeres, Appl. Catal. A: Gen. 449 (2012) 121–130.
[25] M. Bykova, D.Y. Ermakov, V. Kaichev, O. Bulavchenko, A. Saraev, M.Y. Lebedev, V. Yakovlev, Appl. Catal. B: Environ. 113 (2012) 296–307.
[26] M. Bykova, D.Y. Ermakov, S. Khromova, A. Smirnov, M.Y. Lebedev, V. Yakovlev, Catal. Today 220 (2014) 21–31.
[27] A.M. Ruppert, K. Weinberg, R. Palkovits, Angew. Chem. Int. Ed. 51 (2012) 2564–2601.
[28] K. Barta, P.C. Ford, Acc. Chem. Res. 47 (5) (2014) 1503–1512.
[29] K. Tajvidi, K. Pupovac, M. Kükrek, R. Palkovits, ChemSusChem 5 (2012) 2139–2142.
[30] B. Blanc, A. Bourrel, P. Gallezot, T. Haas, P. Taylor, Green Chem. 2 (2000) 89–91.
[31] T.D. Matson, K. Barta, A.V. Iretskii, P.C. Ford, J. Am. Chem. Soc. 133 (2011) 14090–14097.
[32] Y. Wu, F. Gu, G. Xu, Z. Zhong, F. Su, Bioresour. Technol. 137 (2013) 311–317.
[33] C.R. Vitasari, G. Meindersma, A.B. De Haan, Bioresour. Technol. 102 (2011) 7204–7210.
[34] B. Sukhbaatar, Q. Li, C. Wan, F. Yu, E. Hassan, P. Steele, Bioresour. Technol. 161 (2014) 379–384.
[35] F. Arena, K. Barbera, G. Italiano, G. Bonura, L. Spadaro, F. Frusteri, J. Catal. 249 (2007) 185–194.
[36] F. Ronsse, X. Bai, W. Prins, R.C. Brown, Environ. Prog. Sustain. Energy 31 (2012) 256–260.
[37] P.S. Rezaei, H. Shafaghat, W.M.A.W. Daud, Appl. Catal. A: Gen. 469 (2014) 490–511.
[38] A.J. Foster, J. Jae, Y. Cheng, G.W. Huber, R.F. Lobo, Appl. Catal. A: Gen. 423 (2012) 154–161.
[39] T.R. Carlson, J. Jae, Y. Lin, G.A. Tompsett, G.W. Huber, J. Catal. 270 (2010) 110–124.
[40] A.J. Kumalaputri, G. Bottari, P.M. Erne, H.J. Heeres, K. Barta, ChemSusChem (2014), http://dx.doi.org/10.1002/cssc.201402095.
[41] X. Hu, C. Li, Green Chem. 13 (2011) 1676–1679.
[42] W. Li, C. Pan, Q. Zhang, Z. Liu, J. Peng, P. Chen, H. Lou, X. Zheng, Bioresour. Technol. 102 (2011) 4884–4889.
[43] W. Li, C. Pan, L. Sheng, Z. Liu, P. Chen, H. Lou, X. Zheng, Bioresour. Technol. 102 (2011) 9223–9228.
[44] J. Zhang, Z. Luo, Q. Dang, J. Wang, W. Chen, Energy Fuels 26 (2012) 2990–2995.
[45] U.V. Mentzel, S. Shunmugavel, S.L. Hruby, C.H. Christensen, M.S. Holm, J. Am. Chem. Soc. 131 (2009) 17009–17013.
[46] A.G. Gayubo, A.T. Aguayo, A. Atutxa, R. Aguado, M. Olazar, J. Bilbao, Ind. Eng. Chem. Res. 43 (2004) 2619–2626.
[47] J.J. Bravo-Suárez, B. Subramaniam, R.V. Chaudhari, Appl. Catal. A: Gen. 455 (2013) 234–246.
[48] R. Gunawan, X. Li, A. Larcher, X. Hu, D. Mourant, W. Chaiwat, H. Wu, C. Li, Fuel 95 (2012) 146–151.
[49] E. Taarning, C.M. Osmundsen, X. Yang, B. Voss, S.I. Andersen, C.H. Christensen, Energy Environ. Sci. 4 (2011) 793–804.
[50] A. Oasmaa, E. Kuoppala, J. Selin, S. Gust, Y. Solantausta, Energy Fuels 18 (2004) 1578–1583.
[51] M.V. Twigg, Appl. Catal. B: Environ. 70 (2007) 2–15.
[52] T.S. Hansen, K. Barta, P.T. Anastas, P.C. Ford, A. Riisager, Green Chem. 14 (2012) 2457–2461.
[53] M.V. Twigg, M.S. Spencer, Appl. Catal. A: Gen. 212 (2001) 161–174.
[54] J. Barrault, A. Derouault, G. Courtois, J. Maissant, J. Dupin, C. Guimon, H. Martinez, E. Dumitriu, Appl. Catal. A: Gen. 262 (2004) 43–51.